# Positive or negative feedback of optokinetic signals: degree of the misrouted optic flow determines system dynamics of human ocular motor behavior

Chen, Chien-Cheng ; Bockisch, Christopher J ; Olasagasti, Itsaso ; Weber, Konrad P ; Straumann, Dominik ; Huang, Melody Ying-Yu

Abstract: PURPOSE: The optokinetic system in healthy humans is a negative-feedback system that stabilizes gaze: slow-phase eye movements (i.e., the output signal) minimize retinal slip (i.e., the error signal). A positive-feedback optokinetic system may exist due to the misrouting of optic fibers. Previous studies have shown that, in a zebrafish mutant with a high degree of the misrouting, the optokinetic response (OKR) is reversed. As a result, slow-phase eye movements amplify retinal slip, forming a positive-feedback optokinetic loop. The positive-feedback optokinetic system cannot stabilize gaze, thus leading to spontaneous eye oscillations (SEOs). Because the misrouting in human patients (e.g., with a condition of albinism or achiasmia) is partial, both positive- and negative-feedback loops co-exist. How this co-existence affects human ocular motor behavior remains unclear. METHODS: We presented a visual environment consisting of two stimuli in different parts of the visual field to healthy subjects. One mimicked positive-feedback optokinetic signals and the other preserved negative-feedback optokinetic signals. By changing the ratio and position of the visual field of these visual stimuli, various optic nerve misrouting patterns were simulated. Eye-movement responses to stationary and moving stimuli were measured and compared with computer simulations. The SEOs were correlated with the magnitude of the virtual positive-feedback optokinetic effect. RESULTS: We found a correlation among the simulated misrouting, the corresponding OKR, and the SEOs in humans. The proportion of the simulated misrouting needed to be greater than 50% to reverse the OKR and at least greater than or equal to 70% to evoke SEOs. Once the SEOs were evoked, the magnitude positively correlated to the strength of the positive-feedback OKR. CONCLUSIONS: This study provides a mechanism of how the misrouting of optic fibers in humans could lead to SEOs, offering a possible explanation for a subtype of infantile nystagmus syndrome (INS).

DOI: https://doi.org/10.1167/iovs.13-12750

# Positive or negative feedback of optokinetic signals: Degree of the misrouted optic flow determines system dynamics of human ocular motor behavior

Chien-Cheng Chen[1,5], Christopher J. Bockisch[1,2,3], Itsaso Olasagasti[1], Konrad P. Weber[1,2], Dominik Straumann[1,4], and Melody Ying-Yu Huang[1,4]

Departments of [1]Neurology, [2]Ophthalmology, and [3]ENT, University Hospital Zurich, Zurich, Switzerland; the [4]Zurich Center for Integrative Human Physiology (ZIHP), Zurich, Switzerland. [5]PhD Program in Integrative Molecular Medicine, Life Science Graduate School, CH-8057 Zurich, Switzerland

## Abstract

**Purpose.** The optokinetic system in healthy humans is a negative-feedback system that stabilizes gaze: slow-phase eye movements (i.e., the output signal) minimize retinal slip (i.e., the error signal). A positive feedback optokinetic system may exist due to the misrouting of optic fibers. Previous studies have shown that, in a zebrafish mutant with a high degree of the misrouting, the optokinetic response (OKR) is reversed. As a result, slow-phase eye movements amplify retinal slip, forming a positive feedback optokinetic loop. The positive feedback optokinetic system cannot stabilize gaze, thus leading to spontaneous eye oscillations (SEOs). Because the misrouting in human patients (e.g., with a condition of albinism or achiasmia) is partial, both positive/negative feedback loops co-exist. How this co-existence affects human ocular motor behavior remains unclear.

**Methods.** We presented a visual environment consisting of two stimuli in different parts of the visual field to healthy subjects. One mimicked positive feedback optokinetic signals and the other preserved negative feedback optokinetic signals. By changing the projection area of these visual stimuli, various optic nerve misrouting patterns were simulated. Eye-movement responses to stationary and moving stimuli were measured and compared to computer simulations. The SEOs were correlated with the magnitude of the virtual positive feedback optokinetic effect.

**Results**. We found a correlation among the simulated misrouting, the corresponding OKR, and the SEOs in human. The proportion of the simulated misrouting needed to be > 50% to reverse the OKR and at least ≥ 70% to evoke SEOs. Once the SEOs were evoked, the magnitude positively correlates to the strength of the positive-feedback OKR.

**Conclusion**. This study provides a mechanism of how the misrouting of optic fibers in humans could lead to SEOs, offering a possible explanation for a subtype of infantile nystagmus syndrome (INS).

# Introduction

The optokinetic response (OKR) is an eye movement driven by a large moving pattern. The OKR generates slow-phase eye movements following the moving pattern and fast-phase eye movements resetting the eyes to a central position. The optokinetic system is a negative feedback system that reduces the image velocity on the retina (error signal) by keeping the slow-phase eye velocity (output signal) close to the velocity of the visual world[1]. In general, a system with a high degree of negative feedback tends to be stable as it is relatively immune to internal disturbances and automatically compensates for external changes[2]. A positive feedback optokinetic system is rarely found, but may exist due to the misrouting of optic fibers[3,4]. In an achiasmatic zebrafish mutant, in which the misrouting of optic fibers sends optokinetic signals from the retina to the wrong brain hemisphere, the slow phases of the OKR move in the opposite direction of the visual surround, producing a reversed OKR[5]. As a result, retinal slip, the error signal, is amplified by the slow-phase eye velocity, the output signal, forming a positive feedback optokinetic loop. In general, a system with a high degree of positive feedback tends to be unstable as the error signal and the output signal drive the system out of equilibrium[6].

In human patients with misrouted optic fibers, either some of the temporal optic fibers erroneously cross the midline to the contralateral hemisphere, often found in albinos[7-9], or the nasal optic fibers do not cross to the contralateral hemisphere, as in achiasmia[10-12]. Infantile nystagmus syndrome (INS) often accompanies these conditions[13-15]. INS is characterized by spontaneous eye oscillations (SEOs) usually appearing within the first six

months after birth[16], and sometimes co-occurs with a reversed jerk nystagmus during optokinetic stimulation[13,14,17-20]. Recent studies have described a zebrafish mutant that has misrouted optic fibers and displays SEOs qualitatively similar to human INS patients[3,4]. However, approximately one in ten patients with the clinical features of albinism, including the misrouting of optic fibers, show no SEOs[21,22]. Moreover, the existence of reversed OKR in INS patients is debated. While the reversed OKR was reported (based on a reversed nystagmus response) in INS patients[17,18,19,23] and in some albinos[13,14], a reversed nystagmus is not consistently observed in every INS patient. Some have doubted the mechanism of the reversed nystagmus and suggested it is actually gaze-modulated spontaneous nystagmus shifted by optokinetic stimulation[17,24]. Since there are massive inter-individual variations of nystagmus waveforms in INS patients[23,25] as well as variations of waveforms as function of eye position[17,23], it is possible that INS results from several causes in different subpopulations of INS patients. To our knowledge, hypotheses about the origin of INS include connection faults (i.e., the misrouting of optic fibers[3,4]), motor faults[26], abnormal sensorimotor integration[27], and miscalibration of the visual system[24,28]. In this study, we investigated whether the misrouting of optokinetic signals in humans is able to induce SEOs. Specifically, we simulated the misrouting of optic fibres and analyzed the resulting gain of OKR and the velocity of eye oscillations during attempted fixation.

In INS patients with an optic fiber misrouting, it is unlikely that the entire optic projection is aberrant. In most cases, positive- and negative-feedback loops co-exist (Fig. 1). Moreover, the range of misrouting in albinism differs considerably among individuals[29]. In other words, the relative contribution of positive and negative feedback optokinetic systems in human patients varies. In zebrafish, it has been shown that larvae with various degrees of optic nerve misprojections display different corresponding optokinetic behaviors[4]. Therefore, the OKR in human INS patients and the presence of SEOs may differ due to various degrees of abnormal optokinetic feedback as well.

In this study, we created a virtual visual environment to simulate the existence of two different feedback optokinetic loops in healthy subjects. The

experimental environment was created by simultaneously projecting a positive feedback visual stimulus, the velocity of which was controlled based on on-line eye-movement signals to mimic a positive feedback system, and a negative feedback visual stimulus, which preserved the negative feedback system in healthy subjects, in different parts of the visual field. By varying the size and position of the positive/negative feedback stimuli in the visual field, we measured SEOs and OKR in response to various combinations of the two feedback loops. In addition, we used a mathematical optokinetic model to simulate the partial misrouting and compared our empirical data to the modeling results.

## Materials and Methods

### Human subjects

Experiments were performed on eight subjects, aged 23-49 years, with no abnormal neurological or ophthalmological history and normal or corrected-to-normal vision. The study was approved by the Ethics Committee of the Canton of Zürich, Switzerland, and all subjects gave their informed written consent in accordance with the declaration of Helsinki.

### Experimental setup

A head-mounted video-oculography (VOG) device (EyeSeeCam, Munich, German) running at 220 Hz was used for the eye-movement recording. The left eye was analyzed. The subject sat in front of a screen (Gerriets GmbH, Umkirch, Germany) with 178 cm in width and 130 cm in height, which was located 100 cm from the subject. Therefore, it covered 80° of the horizontal visual field and 66° of the vertical visual field. A digital projector (Panasonic PT-AE7000 Projector) operating at 60 frames per second with a spatial resolution of 1920 x 1080 pixels was used to present the visual stimuli. On-line eye-movement recording and analysis were done by commercial software (EyeSeeCam, Munich, Germany). Vertical sine-wave gratings with a spatial frequency of 0.25 cycle/degree and nearly 100% contrast (darkest luminance: 0.17 lux and lightest luminance: 330 lux) were used as the image pattern in both positive and negative feedback visual stimuli. Thus, the visual stimuli were only to test the ocular motor response in the horizontal direction. Image manipulation was done by a custom-developed script in MATLAB (Mathworks,

Natick, MA) and its Psychophysics Toolbox extensions[30-32]. The delay of the external visual feedback setup (i.e., the duration from the eye-movement recording to the visual stimulus manipulation) was approximately 32 ms.

**Positive and negative feedback visual stimuli for the spontaneous eye oscillation (SEO) and optokinetic response (OKR) tests**

To simulate a positive feedback optokinetic system, in which retinal slip increases with eye velocity, the image velocity of the positive feedback visual stimulus was adjusted according to the online eye velocity. Since a negative feedback optokinetic system exists in healthy subjects, the negative feedback visual stimulus did not rely on any real-time eye-movement signal. In the SEO test, we simulated how various combinations of negative and positive feedback loops react to a stationary visual surround. Fig. 2A illustrates how the image motions of two feedback visual stimuli were controlled in this test. If eye movements existed, retinal slip (i.e., the error signal of the negative-feedback system) would be the negative of eye velocity because the image velocity was zero. But the error signal of the positive feedback optokinetic system would be equal to eye velocity due to a reversed OKR. To simulate such a positive feedback condition in healthy subjects, the image velocity was set to the double real-time eye velocity in the positive feedback condition. The error signal, then, would be the same value as the real-time eye velocity and a virtual positive feedback system was created.

In the OKR test, we simulated how various combinations of two feedback loops react to a globally moving visual surround. Fig. 2B illustrates how the image motions of two feedback visual stimuli were controlled in this test. A constantly moving image pattern (20 deg/s) was applied in the negative feedback condition. A similar calculation as described in the SEO test was then applied to obtain the image velocity in the positive feedback condition. Since the positive feedback visual stimulus required the real-time eye-movement information, we used the real-time horizontal left-eye movements as a feedback signal. Vertical eye movements were neglected since both of positive/negative feedback visual stimuli were controlled to only move horizontally.

The velocity of all stimuli was not spatially adjusted when projecting on the flat screen. In other words, if the stimulus moved at constant velocity, it did

move at constant pixels per second. The velocity of visual stimuli was calculated by averaging the stimulus velocity on the central 10° visual field.

**Experimental paradigms**

In each paradigm, the central visual field (ranging from 10° to 80°) received one visual stimulus while the eccentric regions (from the edge of the central stimulus to the edge of the screen at +/- 40°) received the other stimulus (Fig 3A and Fig. 4A). If the positive feedback visual stimulus was projected to the central visual field, the negative feedback visual stimulus would be shown in the peripheral visual field, and vice versa. The boundaries of the central visual field were symmetric around gaze straight ahead and moved with the left eye. If the border of the central field stimulus crossed the edge of the screen, the border would be set on the edge of the screen while the other border kept moving with eyes. Relative positions of two boundaries and eyes were obtained by using the inverse tangent function taking accounts of the distance between eyes and the flat screen. Thus, the visual stimuli were always on the same area of the retina unless the area of the visual stimuli was out of the projection range. During the tests, subjects were asked to look about straight ahead, but to let their eyes move in response to the visual stimuli. Each paradigm lasted for 30 seconds, and there was a 10-second break between paradigms. During the break, subjects were asked to stare at a fixed dot on the center of the screen, and at the same time, move his/her head to drive another moving dot, which moved with the real-time eye-in-head position to overlap with the stationary dot at the center of the screen. The dots would overlap if the head and eye-in-head positions were straight ahead, ensuring that the head position was the same at the beginning of each trial. All subjects were able to fix the moving dot to the center of the screen within the 10-second break. Also, subjects were instructed to keep their head still during each trial, and head position was monitored by the experimenter. Thus, the head movement as well as the head position would not play an important role on the experimental outputs.

**Computational modeling**

Computer simulations done in MATLAB Simulink (Mathworks, Natick, MA) were compared to the empirical data. The model consists of a visual input

generator and an optokinetic model (Fig. 6A). The optokinetic model is the sum of the positive and negative feedback optokinetic models, with a parameter, R, which controls the relative weighting of the two models. The negative feedback optokinetic model used here was first published by D. A. Robinson[1] and has been further modified to be closer to the human OKR (see Supplemental Material). The positive feedback model was obtained by adding a gain block of minus one after the block delay in the retina (see Supplemental Material). R (ranging from 0 to 1) indicates the proportion of the positive feedback optokinetic systems. The motor commands from the whole model are added to obtain the final motor response. To simulate the SEO test, a small impulse (of 1 deg/s for 1 s) was given at the beginning of the simulation. To simulate the OKR test, a constant input signal (20 deg/s) was applied.

**Data analysis**

Data analysis was done with a custom-developed program written in MATLAB (Mathworks, Natick, MA). Eye position was smoothened by a Gaussian low-pass filter with a cut-off frequency of 18 Hz. Eye velocity was computed by the derivative of eye position. The median absolute eye velocity in the SEO test and the median eye velocity in the OKR test were calculated to represent the magnitude of the SEOs and the degree of stability of the optokinetic system. In the SEO and OKR test, a statistical test (t-test) was done in each subject and the whole group to examine whether an effect exists between the eye-movement response and the visual feedback type of central visual field while another statistical test (one-way ANOVA) was done in each subject as well as the whole group to examine whether there is a main effect between the eye-movement response and the size of the central field stimulus. Moreover, regression lines of eye velocity versus the size of the central area were computed in each subject and the whole group. These linear fits allow us to determine, for each subject and the whole group, if eye velocity increased with stimulus area (that is, with the ratio of positive-to-negative feedback). In addition, the correlation (Pearson's product moment correlation) between the eye velocities in the SEO and OKR tests was calculated. Statistical tests were done in MATLAB with the Statistics Toolbox (Mathworks, Natick, MA).

## RESULTS

**Spontaneous eye oscillation (SEO)**

The SEO test was applied to mimic how various combinations of positive and negative feedback loops react to a stationary stimulus. The velocity of the negative feedback stimulus in the SEO test was set to zero so that retinal slip decreased with eye velocity, i.e. the negative feedback loop. The velocity of the positive feedback stimulus in the SEO test was set to the double real-time eye velocity so that retinal slip increased with eye velocity, i.e. the positive feedback loop (Fig. 2A). Fig. 3B shows the eye movements of one subject under all stimulus combinations. This subject generated SEOs when the positive feedback visual stimulus was shown in the central visual field (right column), but no SEO was found when the negative feedback visual stimulus was in the central visual field (left column). Fig 3C shows the median absolute slow-phase eye velocity of all subjects in all conditions.

Seven of 8 subjects showed a significant eye-velocity difference between the visual feedback types of central visual field (t-test, all ps<0.05 in these 7 subjects). Overall, the average(±SD) velocity of the central visual field stimulus of positive feedback (Fig. 3C, right part) was 5.6±4.0 deg/s, significantly different to the one of the central visual field stimulus of negative feedback (Fig. 3C, left part), which was 0.6±0.5 deg/s (t-test, p<0.0001). Moreover, when the positive feedback visual stimulus was shown in the central visual field, 6 of 8 subjects showed statistically increasing eye velocity with stimulus area (average(±SD) slope = 0.0991(±0.0247) (deg/s)/deg; One-way ANOVA, all ps<0.05 in these 6 subjects), whereas in the negative feedback condition, none of the subjects showed a significant change in eye velocity with stimulus area (average(±SD) slope = 0.0004(±0.0016) (deg/s)/deg; One-way ANOVA, all ps>0.05 in all subjects). Overall, the median eye velocity increased with the size of the central visual field stimulus of positive feedback ($R^2$ = 0.2473; One-way ANOVA, $F_{(1,38)}$=12.49, p=0.0011), but no correlation was found between the median eye velocity and the size of the central visual field stimulus of negative feedback ($R^2$ = 0.0337; One-way ANOVA, $F_{(1,38)}$=1.33, p=0.2569). In general, the beating field in all subjects during the SEO test was in the range of +/-20°, so the central projection a rea, which moved with left eye,

did not go beyond the screen borders much when its size was less than 50°.

Three INS-like subtypes of SEOs[25] were found during the SEO tests. Most waveforms were similar to pure unidirectional jerk nystagmus or unidirectional jerk nystagmus with extended foveation periods, in which the slow phases mainly moved in one direction (see Fig. 3B for example, right part except the bottom). Two subjects generated bidirectional pseudo-pendular nystagmus, in which the slow phases changed the direction regularly after saccades, when the positive feedback visual stimulus was only in the central 10° visual field (see Fig 3B for example, central area 10°). The frequency of SEOs approximately ranged between 0.3 and 0.7 Hz but varied a lot in subjects as well as the stimulus combinations (see Fig. 3B).

**Optokinetic response (OKR)**

The OKR test was applied to test how various combinations of positive and negative feedback loops react to a moving visual surround. The velocity of the negative feedback stimulus in the OKR test was set to 20 deg/s to the left. If eyes followed the negative feedback stimulus, retinal slip would decrease. The velocity of the positive feedback stimulus in the OKR test was set to 20 deg/s plus the double real-time eye velocity (Fig. 2B). In this positive feedback condition, retinal slip increased even when eyes followed the positive feedback stimulus. Fig. 4B shows the eye movements of one subject under all stimulus combinations. We found that slow phases followed the image motion presented in the central visual field, but that the magnitude of slow-phase eye velocity differed. Fig 4C shows the median eye velocity of all subjects in all conditions.

All 8 subjects showed a significant eye-velocity change regarding the visual feedback type of central visual field (t-test, all ps<0.05 in all subjects). Overall, the average(±SD) velocity of the central visual field stimulus of positive feedback (Fig. 4C, right part) was -6.2±4.0 deg/s, significantly different to the one of the central visual field stimulus of negative feedback (Fig. 4C, left part), which was 6.9±5.0 deg/s (t-test, p<0.0001). When the positive feedback visual stimulus was in the central visual field, 6 of 8 subjects showed statistically eye-velocity increasing with the size of stimulus area (average(±SD) slope =

-0.1257(±0.0389) (deg/s)/deg, all ps<0.05 in these 6 subjects). In the negative feedback conditions, in most subjects, eye velocity seemed to be saturated when the central area was still small, and then did not increase further. Thus, only 2 subjects showed statistically increasing eye-velocity with stimulus area (average(±SD) slope = 0.1555(±0.0094) (deg/s)/deg, all ps<0.05 in these 2 subjects). Overall, however, the magnitude of the median eye velocity increased with the size of the central visual field stimulus of positive feedback ($R^2$ = 0.5297; $F_{(1,38)}$=42.79, p<0.0001) and negative feedback ($R^2$ = 0.2005; $F_{(1,38)}$=9.52, p=0.0038). In general, the beating field in all subjects during the OKR test was in a range of +/-20°, so the central p rojection area, which moved with left eye, did not go beyond the screen borders much when its size was less than 50°.

**Comparison between the SEO and OKR tests.**

A stimulus combination represents a kind of co-existence of two feedback loops and its gaze stability and OKR were tested in the SEO and OKR tests, respectively. If the stimulus combinations in the OKR test caused slow phases to follow the negative feedback visual stimulus, gaze should be stable due to the stability of the negative feedback optokinetic loop. From the experimental results, we found that no SEO occurred (Fig 4C, left) when slow phases followed the negative feedback visual stimulus (Fig 3C, left). If the stimulus combinations caused slow phases to move in the direction of the positive feedback visual stimulus, the SEOs were expected to occur due to the instability of the positive feedback optokinetic loop. However, one subject (●) had no or weak SEO (Fig 3C, right) with the stimulus combinations where his eyes followed the positive feedback visual stimulus (Fig 4C, right). Moreover, three subjects generated obvious SEOs only if the size of the central visual field was ≥ 50° (Fig 3C, right part). Such an unexpected resul t, which challenges the hypothesis that the instability necessarily evokes SEOs, raises a question: how does the positive feedback optokinetic loop relate to the SEOs?

To find out the relation between the SEOs and the positive feedback optokinetic loop, we then correlated the eye velocity obtained with the positive

feedback stimulus in the central field in the OKR test (Fig 4C, right) with the corresponding data from the SEO test (Fig 3C, right). The correlation (Fig. 5) was significantly positive (Pearson linear coefficient of 0.6337, $p<0.0001$).

**Computer simulation**

Computer simulations were done for a comparison with the empirical data, using several different OKR gain curves (see Supplemental Material). In the simulated SEO test (Fig 6B), the simulated eye velocity of the normal gain OKR curve starts to increase when the proportion of fiber misrouting is ≥ 0.7. For the two lower gain OKR curves, a higher proportion of simulated misrouting is needed to induce the simulated SEOs. Once the simulated SEOs are evoked, the magnitude increases with the proportion of misrouted fibers. For the two lowest OKR curves, no SEO is generated. In the simulated OKR test (Fig. 6C), the simulated OKR velocity is highest when there is no misrouted fiber. Then the simulated OKR velocity decreases with the proportion of the simulated optic fiber misrouting. When the proportion of the simulated optic fiber misrouting is 0.5, the simulated OKR velocity of all OKR gain curves becomes zero. Above 0.5, the OKR reverses for all curves.

We also tried to find out the relation between the simulated gaze stability, which was tested in the simulated SEO test, and the simulated OKR, which was tested in the simulated OKR test, in order to be a comparison with the analysis shown in Fig. 5. If the eye-velocity output is in the same direction of the visual input, the negative feedback optokinetic loop dominates so that gaze should be stable. From the modeling results, we found that no simulated SEO occurs (Fig 6B, the data with a proportion < 0.5) when the eye-velocity output is in the same direction of the visual input (Fig 6C, the data with a proportion < 0.5). If the eye-velocity output is in the opposite direction of the visual input, the simulated SEOs should occur due to the instability of the positive feedback optokinetic loop. However, similar to the experimental results, no occurrence of the simulated SEO is possible (Fig 6B, the data with a proportion > 0.5) when the simulated output is reversed (Fig 6C, the data with a proportion > 0.5). We correlated the magnitude of the simulated OKR velocity of a positive-feedback-dominated system (Fig 6C, right part) with the corresponding data from the simulated SEO test (Fig 6B, right part). Similar to

Fig. 5, the correlation (Fig. 7) was significantly positive (Pearson linear coefficient of 0.7855, $p < 0.0001$). However, rather than the linear relation between the two, it is more likely that the occurrence of the simulated SEOs requires instability more than certain degree as well as relies on the individual OKR.

## Discussion

In this study, we investigated how the simultaneous existence of positive and negative optokinetic feedback loops affects the optokinetic response (OKR) as well as fixation stability. The optokinetic system in healthy humans is a negative feedback system, in which retinal slip is reduced by keeping the slow-phase eye velocity close to the velocity of the visual world[1]. The positive feedback system, in which retinal slip increases with slow-phase eye movements, may be created by the misrouting of optic fibers. Our earlier studies in zebrafish larvae[3-5] demonstrated that the OKR in achiasmatic mutant zebrafish larvae is reversed, forming a positive feedback optokinetic system. In these fish, spontaneous eye oscillations (SEOs) are often observed[3,4]. Although no correlation study among the misrouting of optic fibers, the reversed OKR, and the SEOs has been done in human yet, an earlier study[29] found that the space organization in the visual cortex of the misrouting of optic fibers re-arranges in the way of horizontal mirror symmetry (Fig. 1A). Such a mirror-symmetrical arrangement may produce a positive feedback loop in the optokinetic system (Fig. 1B). Moreover, the reversed nystagmus during optokinetic stimulation was found to occur in some patients with infantile nystagmus syndrome (INS)[17-19] and albinism[13,24] although its true mechanism was doubted as well[24]. We mimicked the simultaneous existence of positive and negative optokinetic feedback loops in healthy subjects and measured the change in the OKR as well as fixation stability for a better control. The positive and negative feedback loops were experimentally achieved by performing real-time control of image motion based on on-line eye-movement recordings in each subject (Fig. 2). The relative amount of fiber misrouting was simulated by adjusting the stimulated retinal areas of the two feedback stimuli (Fig. 3A and 4A). Moreover, computer simulations with the different proportions of the simulated optic fiber misrouting were applied as a comparison with the

empirical data (Fig. 6).

From the experimental results, a significant difference of visual feedback type in the central visual field was found. The fixation stability was preserved in the SEO test (Fig. 3C, left) and slow phases followed the negative feedback visual stimulus in the OKR test (Fig. 4C, left) as long as the negative feedback visual stimulus was in the central visual field, suggesting that a negative feedback optokinetic system, irrespective of its magnitude, can effectively stabilize gaze. When the positive feedback visual stimulus was in the central visual field, the occurrence of SEOs in the SEO test seemed to rely on the individual response as well as the stimulus combination (Fig. 3C, right) but slow phases in all subjects in the OKR test followed the positive feedback visual stimulus (Fig. 4C, right), suggesting that a positive feedback optokinetic system has a capacity to evoke SEOs. Both the magnitude of the SEOs and the degree of the positive feedback OKR significantly increased with the size of the central field stimulus, suggesting that a higher degree of misrouted optokinetic signals can form a stronger positive feedback optokinetic system, which further induces more intense SEOs. The correlation between the degree of the positive feedback optokinetic system and the magnitude of the SEOs was significantly positive (Fig. 5).

In our computer simulations, if the negative feedback optokinetic system dominates (i.e. a proportion of the simulated optic fiber misrouting < 0.5), no simulated SEO occurs (Fig. 6B) and the simulated OKR is normal (in terms of direction) (Fig. 6C), similar to what we found in the experimental results. If the positive feedback optokinetic system dominates (i.e. a proportion > 0.5), the simulated OKR is reversed (Fig. 6C) but the simulated SEOs occur only if the proportion of the simulated optic fiber misrouting is at least 0.7 (Fig. 6B). Once the simulated SEOs are evoked, the magnitude increases with the proportion of the misrouting. However, even when proportion of the misrouting is the same, the simulated SEOs can be smaller or may not occur, with a lower gain OKR curve (Fig. 6B). We further correlated the degree of the simulated reversed OKR with the corresponding fixation stability (Fig. 7). Similar to Fig. 5, the correlation is significantly positive. However, rather than a linear relation between these two, it is more likely that the simulated SEOs need to be

triggered by certain degree of instability first and then the magnitude increases with the degree of the simulated reversed OKR.

By comparing the experimental results (Fig. 5) with the simulation (Fig. 7), we found a disagreement as to whether a low degree of the instability is able to evoke SEOs. In our simulation, the simulated SEOs need to be triggered by certain degree of instability. However, the experimental results showed that the SEOs were able to be evoked by a weak instability. We speculate that such SEOs may result from an involvement of smooth pursuit. The stimulus combinations that caused such weak instability but obvious SEOs were that the positive feedback visual stimulus was in the central 10° or 20° visual field, which contains the fovea. The central projection area moved consistently with left eye to make sure that the central field stimuli were always in the same area of the retina. Such a condition may somehow activate the smooth pursuit system to follow the moving central visual field and induce SEOs.

The between-subject variations were large in the SEO and OKR tests (Fig. 3C and 4C). Two subjects showed relatively weak eye movements under all paradigms. Even with the stimulus combination that the negative feedback (constantly moving) optokinetic stimulus was in the central 80° visual field, their eye velocities were still low (Fig. 4C, left most condition), suggesting that these two subjects have a naturally low OKR. Therefore our paradigms, which mainly affected the optokinetic system, were not able to significantly change their ocular motor behavior. Moreover, from the computational simulation, we found that the simulated SEOs may vary considerably by just dividing the normal OKR curve by 1.2 and 1.3. With a further lower OKR curve, the simulated SEO do not occur (Fig. 6B). The simulated results support that the large between-subject variation found in Fig. 3C and 4C resulted from the individual difference rather than the experimental design.

**OKR-related visual field.**

From the experimental results, we found eyes followed the stimulus in the central 10° visual field, even when the area of stimulation of the peripheral field was substantially larger and the stimulus of the peripheral field was conflicting to the one of the central field (Fig. 4C, the central two conditions), suggesting

that the optokinetic signals of the central 10° visual field were weighted more than the signals from the peripheral field. This finding is consistent with numerous studies that showed the central retina is more effective in driving the OKR[33-36].

We expect that the magnitude of the median eye velocity should significantly increase with the size of the central field stimulus simply because a larger area of the central field carries more optokinetic signals while the conflicting optokinetic signals from the peripheral field is less. Based on the experimental results, we found that the median eye velocity, overall, significantly increased with the size of the central field stimulus, irrespective of the feedback type in the central field (Fig. 4C). However, the linear fits of the median eye velocity and the area of the central field stimulus of negative feedback was significantly positive in only two subjects (Fig. 4C, left part). With a careful look at the left part of Fig. 4C, most of subjects only showed a subtle change when the area of the central field was more than 30°, suggesting that the central 30° visual field carries most of optokinetic signals. However, such a saturation effect was not found when the positive feedback visual stimulus was in the central field (Fig. 4C, right part). This could be because the image velocity of the positive feedback visual stimulus increased with eye velocity. Therefore, in such a positive feedback condition, the visual field effect could be affected so that the saturation effect was not found.

**Waveform analysis.**

Waveforms in the SEO tests are highly reliant on the initial retinal slips as well as the interaction of the feedback stimulus and the optokinetic system. The SEOs in most subjects were unidirectional. From the view of system dynamics, the unidirectional SEOs can be explained as a result of a strong positive feedback loop. The initial retinal slip, induced by either slight self-rotation or a subtle oscillation of visual surround, is random and can be in either direction. The initial retinal slip, then, is magnified and maintained by the high degree of positive feedback. Thus the eyes keep moving in one direction and unidirectional SEOs occur.

Bidirectional SEOs were found only in two subjects with the stimulus

combinations that the positive feedback visual stimulus was in the central 10° visual field. The mechanism responsible for the bidirectional SEOs may be a weak instability of the optokinetic system and an involvement of smooth pursuit. According to the experimental results (Fig. 4C), the central 10°field stimulus of positive feedback can only cause the OKR to become slightly unstable, which is unable to evoke a SEO based on the simulation readout (Fig. 6BC and Fig. 7). However, with the weak instability, eyes were no longer restrained by the optokinetic system and were free to move around. Then, the smooth pursuit might be activated by the central visual field, which moved with eyes consistently to keep the central field stimulus approximately on the same area of the retina (see experimental paradigms of Materials and Methods). If the interaction between the smooth pursuit and the central visual field happened to change the direction regularly after each saccade, the bidirectional SEOs would occur, like the lowest one of the right part in Fig. 3B.

**Relation to infantile nystagmus syndrome (INS)**

Human patients with misrouted optic fibers, such as those with albinism[7-9] and achiasmia[10-12], often have infantile nystagmus syndrome (INS)[13-15] that is characterized by SEOs appearing within six months after birth[16]. This study provides a possible mechanism of how misrouting leads to SEOs. If the misrouting creates a strong positive feedback loop, SEOs are likely to occur. This study also indicates that gaze can be stable if the misrouting is not large enough to reverse the OKR or the OKR is reversed but too weak to evoke SEOs, explaining why some patients with misrouted optic fibers have stable gaze[21,22]. Our results in normal subjects also suggest that SEOs will not occur if the OKR gain is low. Moreover, a reversed OKR, a main characteristic of the positive feedback optokinetic system, can be used as a clinical test of whether INS is related to abnormal optokinetic feedback. If SEOs are linked to abnormal optokinetic feedback, then both the OKR and the resulting nystagmus should be reversed. If INS patients do not have a reversed OKR, their nystagmus may or may not reverse and their SEOs should be due to other pathological deficits[24,26-28.].

A prominent INS characteristic, nystagmus in the dark[37], cannot be explained by this study. Also, frequency of SEOs in INS patients, ranged

between 3 and 6 Hz[37,38], is much higher to what we observed in this study. In our study, our subjects only experience each stimulus for 30 seconds, so adaptive mechanisms were unlikely to contribute to the measured response, unlike in patients. Easter and Schmidt[39] found that goldfish with artificially induced ipsilateral retinal projections showed spontaneous nystagmus and reversed OKR. After long-lasting nystagmus in the light, the nystagmus was found to exist in the dark. In the same study, they also found that the fish began to circle after regeneration of the deflected optic nerves and the speed of circling, which is supposed to be related to the magnitude of the spontaneous nystagmus in fish, increased over weeks. If what happened in fish was also true in human, the mismatch between the INS patients and this study may be explained. However, whether such adaptation plays a role in human INS is speculative, does not explain INS in dark at birth, and requires further investigation.

## Reference


[1] Robinson DA. The use of control systems analysis in the neurophysiology of eye movements. *An. Rev Neurosci*. 1981;4: 463-502.

[2] Black HS. Stabilized Feedback Amplifiers. *Bell System Tech J.* 1934;13: 1–18.

[3] Huang YY, Rinner O, Hedinger P, Liu SC, et al. Oculomotor instabilities in zebrafish mutant belladonna: a behavioral model for congenital nystagmus caused by axonal misrouting. *J Neurosci.* 2006;26: 9873–9880.

[4] Huber-Reggi SP, Chen CC, Grimm L, et al. Severity of infantile nystagmus syndrome-like ocular motor phenotype is linked to the extent of the underlying optic nerve projection defect in zebrafish belladonna mutant. *J Neurosci.* 2012;32:18079-86.

[5] Rick JM, Horschke I, Neuhauss SC. Optokinetic behavior is reversed in achiasmatic mutant zebrafish larvae. *Curr Biol.* 2000;10:595–598.

[6] Zeigler BP, Praehofer H, Kim TG. Theory of Modeling and Simulation: Integrating Discrete Event and Continuous Complex Dynamic Systems. *New York: Academic Press.* 2000.

[7] Lund RD. Uncrossed visual pathways of hooded and albino rats. *Science.* 1965;149:1506–1507.

[8] Jeffery G. The albino retina: an abnormality that provides insight into normal retinal development. *Trends Neurosci*. 1997;20:165–169.

[9] Morland AB, Hoffmann MB, Neveu M,et al. Abnormal visual projection in a human albino

studied with functional magnetic resonance imaging and visual evoked potentials. *J Neurol Neurosurg Psychiatry*. 2002;72:523–526.

[10] Apkarian P, Bour LJ, Barth PG, et al. Non-decussating retinal-fugal fibre syndrome. An inborn achiasmatic malformation associated with visuotopic misrouting, visual evoked potential ipsilateral asymmetry and nystagmus. *Brain*. 1995;118:1195–1216.

[11] Petros TJ, Rebsam A, Mason CA. Retinal axon growth at the optic chiasm: to cross or not to cross. *Annu Rev Neurosci.* 2008;31:295–315.

[12] Hoffmann MB, Kaule FR, Levin N, et al. Plasticity and Stability of the Visual System in Human Achiasma. *Neuron*. 2012;75:393-401.

[13] Collewijn H, Apkarian P, Spekreijse H. The oculomotor behaviour of human albinos. *Brain*. 1985;108:1–28.

[14] St John R, Fisk JD, Timney B, et al. Eye movements of human albinos. *Am J Optom Physiol Opt*. 1984;61:377–385.

[15] Biega TJ, Khademian ZP, Vezina G. Isolated absence of the optic chiasm: a rare cause of congenital nystagmus. *AJNR Am J Neuroradiol*. 2007;28: 392–393.

[16] Von Noorden GK, Campos EC. *Binocular Vision and Ocular Motility*. Mosby. St. Louis; 2002;508–533.

[17] Halmagyi GM, Gresty MA, Leech J. Reversed optokinetic nystagmus (OKN): mechanism and clinical significance. *Ann. Neurol*. 1980;7:429–435.

[18] Yee RD, Baloh RW, Honrubia V. Study of congenital nystagmus: optokinetic nystagmus. *Br J Ophthalmol*. 1980;64: 926–932.

[19] Lueck CJ, Tanyeri S, Mossman S, Crawford TJ, and Kennard C. Unilateral reversal of smooth pursuit and optokinetic nystagmus. *Revue Neurologique (Paris)*. 1989;145, 656-660

[20] Thurtell MJ, Leigh RJ. Nystagmus and saccadic intrusions. *Handb Clin Neurol*, 2011;102:333-378.

[21] Lee KA, King RA, Summers CG. Stereopsis in patients with albinism: clinical correlates. *J AAPOS*. 2001;5:98-104.

[22] Gradstein L, FitzGibbon EJ, Tsilou ET, et al. Eye movement abnormalities in Hermansky-Pudlak syndrome. *J AAPOS*. 2005;9:369-378

[23] Oh SY, Shin BS, Jeong KY, Hwang JM, Kim JS. Clinical and Oculographic Findings of X-linked Congenital Nystagmus in Three Korean Families. J Clin Neurol. 2007;3:139-146.

[24] Jacobs JB, Dell'Osso LF. Congenital nystagmus: hypotheses for its genesis and complex waveforms within a behavioral ocular motor system model. *J Vis*. 2004:4:604-25.

[25] Dell'Osso LF, Daroff RB. Congenital nystagmus waveforms and foveation strategy. *Doc Ophthalmol*. 1975;39:155–182.

[26] Dell'Osso LF. Biologically relevant models of infantile nystagmus syndrome: the requirement for behavioral ocular motor system models. *Semin Ophthalmol*. 2006;21:71–77.

[27] Harris C, Berry D. A developmental model of infantile nystagmus. Semin Ophthalmol. 2006;21:63–69.

[28] Anderson JR. Causes and treatment of congenital eccentric nystagmus. Br J Ophthalmol. 1953;37:267–281.

[29] Hoffmann MB, Tolhurst DJ, Moore AT, et al. Organization of the visual cortex in human albinism. *J Neurosci.* 2003;23:8921–8930.

[30] Brainard DH. The Psychophysics Toolbox. *Spat Vis*. 1977;10:433-6.

[31] Pelli DG. The VideoToolbox software for visual psychophysics: transforming numbers into movies. *Spat Vis*. 1977;10:436-442.

[32] Kleiner M, Brainard D, Pelli D, et al. What's new in Psychtoolbox-3. *Perceptio.* 2007;36:1-1.

[33] Cheng M, Outerbridge JS, Optokinetic nystagmus during selective retinal stimulation. *Exp Brain Res*. 1975;23:129-139.

[34] Van Die G, Collewijn H. Optokinetic nystagmus in man. Role of central and peripheral retina and occurrence of asymmetries. *Hum Neurobiol*. 1982;1:111-119.

[35] Howard IP, Ohmi M. The efficiency of the central and peripheral retina in driving human optokinetic nystagmus. *Vision Res*. 1984;24:969-976.

[36] Abadi RV, Howard IP, Ohmi M, Lee EE. The effect of central and peripheral field stimulation on the rise time and gain of human optokinetic nystagmus. *Perception. 2005;34:1015-1024.*

[37] Hertle RW, Dell'Osso LF. Nystagmus in Infancy and Childhood: Current Concepts in Mechanisms, Diagnoses, and Management. *Oxford University Press, New York*. 2013; 1-323.

[38] Kumar A, Gottlob I, Mclean RJ, et al. Clinical and oculomotor characteristics of albinism compared to FRMD7 associated infantile nystagmus. *Invest Ophthalmol Vis Sci*. 2011;52:2306-13.

[39] Easter SS, Schmidt JT. Reversed visuomotor behavior mediated by induced ipsilateral retinal projections in goldfish. *J neurophysiol.* 1977;40:1245-1254.

## Acknowledgements

The authors like to thank Marco Penner and Urs Scheifele for excellent technical assistance. This work was supported by the Swiss National Science Foundation (SNF) grants PMPDP3_139754 (Marie Heim-Vögtlin programme) & 31003A-118069, Zurich Center for Integrative Human Physiology (ZIHP), and Betty and David Koetser Foundation for Brain Research.

## Legends

**FIGURE 1.** Schematic (**A**) and the sign of optokinetic flow (**B**) of the projection of the temporal and nasal retina of left eye in a healthy control (left) and a subject patient with misrouting of optic nerves (right). (**A**) This figure is adapted from Hoffmann et al. (2003). Briefly, in the top row of Fig. 1a, schematic of the stimuli (the gray gradient map) in the visual field is shown. In the second row, the projection of optic nerves from temporal and nasal retina is presented. In the third row, the mapping on the visual cortex is shown with the gray gradient map. In the healthy control, the gray gradient mapping represents the corresponding space organization in the visual cortex. In the patient with misrouting of optic nerves as shown in this figure, part of the cortical input from the temporal retina is misrouted onto the right hemisphere. The corresponding space organization in the visual cortex from the misrouted optic nerves, then, presents in the way of horizontal mirror symmetry (upper part) and superimposes on the normal input from the nasal retina (lower part). (**B**) In the control, all of the optic flow is channeled to the negative feedback loop. But in the patient with misrouting of optic nerves, the horizontal mirror arrangement of the misrouting of optic nerves reverses the negative feedback loop to a positive feedback loop. R represents proportion of optic fiber misrouting.

**FIGURE 2.** The image velocity of the positive- and negative-feedback visual stimuli in the spontaneous eye-oscillations/optokinetic response tests. (A) In the spontaneous eye-oscillations test, stationary gratings were presented as the negative-feedback visual stimulus. In the healthy subject, the error signal is the negative of eye velocity if any eye movement occurs (first column). But in the patient with the positive-feedback optokinetic loop, the error signal is eye

velocity (second column). To mimic the positive-feedback condition in healthy subjects, the image velocity was set to the double eye velocity (third column). (B) In the optokinetic response test, constant optokinetic velocity of 20 deg/s was presented as the negative-feedback visual stimulus. In the healthy subject with the negative-feedback optokinetic loop, the error signal is the optokinetic velocity minus eye velocity (first column). But in the patient with the positive-feedback optokinetic loop, the error signal is the optokinetic velocity plus eye velocity (second column). To mimic this positive-feedback condition in healthy subjects, the image velocity should be equal to the optokinetic velocity with the reversed sign plus the double eye velocity (third column).

**FIGURE 3.** Visual stimulus conditions and results of the spontaneous eye-oscillations test. (**A**) Expression of the presented visual condition is shown in the 2x3 table. In the example, the positive feedback visual stimulus is projected onto the central visual field while the negative feedback visual stimulus is projected on the rest of the screen. θ is the size of the central area. (**B**) Eye movements of one subject under different stimulus combinations. The combinations of the central field stimulus of negative feedback are shown in the left column while the ones of the central field stimulus of positive feedback are shown in the right column. Different rows are different θs. (**C**) Median absolute eye velocity of eight subjects under all stimulus combinations. The stimulus combinations, which are indicated by the tables and θs below referred to panel A of this figure, are shown in the abscissa. The ordinate is eye velocity.

**FIGURE 4.** Visual stimulus condition and results of the optokinetic response test. (**A**) The projection conditions are the same as the ones in the spontaneous eye-oscillations test but with the visual stimuli calculated in Fig. 2B. (**B**) Eye movements of one subject under different stimulus combinations. The combinations of the central field stimulus of negative feedback are shown in the left column while the ones of the central field stimulus of positive feedback are shown in the right column. Different rows are different θs. (**C**) Median absolute eye velocity of eight subjects under all stimulus combinations. These combinations are indicated by the tables and θs listed below. The stimulus combinations, which are indicated by the tables and θs referred to

panel A of this figure, are shown in the abscissa. The ordinate is eye velocity.

**FIGURE 5.** Correlation between the results of the SEO and OKR tests. Data points were obtained by grouping data points on the right part of Fig. 3C and Fig. 4C. For instance, if one subject showed a median eye velocity of -4.6 deg/s in the OKR test and an absolute median eye velocity of 8 deg/s in the SEO test, when the positive feedback visual stimulus was showed on the central 20° visual field, a data point (4.6, 8) was obtained. Note we only took the absolute value, which represents the degree of instability. The solid black line is a linear regression fit of the data. The degree of instability was positively correlated to the magnitude of the SEOs (Pearson's linear correlation coefficient $r=0.6337$, $P<0.0001$).

**FIGURE 6.** Computer simulation. (**A**) Schematic of the optokinetic model is shown. R represents proportion of the simulated optic fiber misrouting. (**B**) Results of the simulated SEO test. (**C**) Results of the simulated OKR test.

**FIGURE 7.** Correlation between the results of the simulated SEO and OKR tests with the data of a proportion > 0.5. Data points were obtained by grouping data points on the right part of Fig. 6B and Fig. 6C. The correlation was significantly positive (Pearson linear coefficient of 0.7855, $p < 0.0001$).

**Figure 1.**

**A**

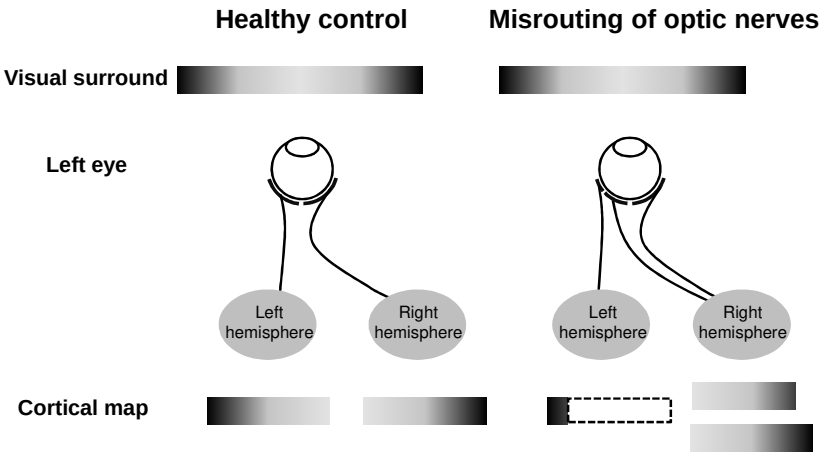
Healthy control
Misrouting of optic nerves
Visual surround
Left eye
Left hemisphere
Right hemisphere
Left hemisphere
Right hemisphere
Cortical map

**B**

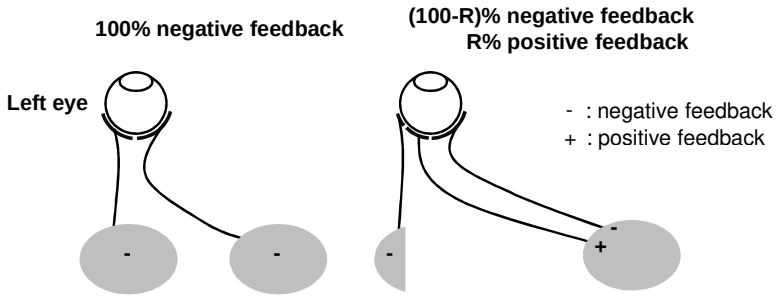
100% negative feedback
(100-R)% negative feedback
R% positive feedback
Left eye
- : negative feedback
+ : positive feedback
-
-
-
-
+

**Figure 2.**

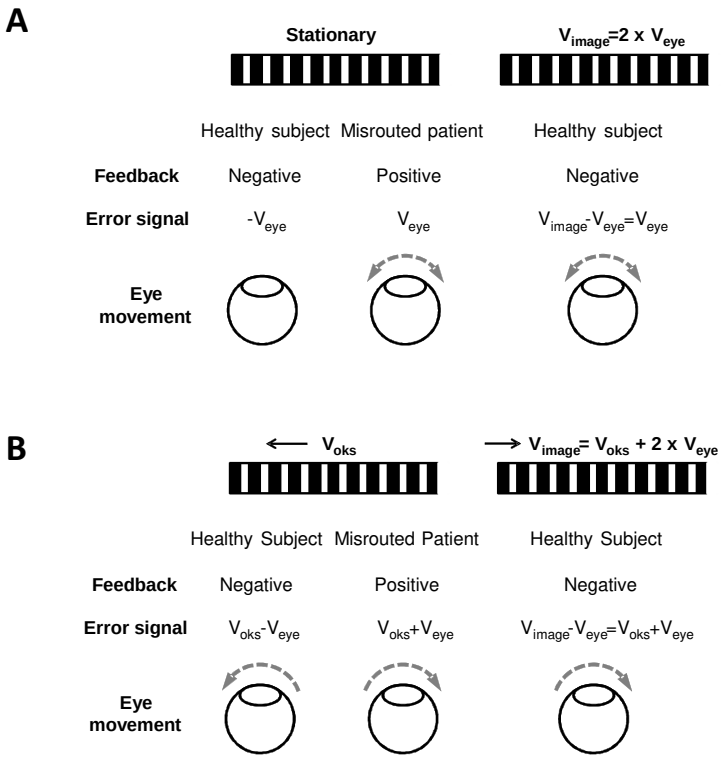
A
Stationary
$V_{image}=2 \times V_{eye}$
Healthy subject
Misrouted patient
Healthy subject
Feedback
Negative
Positive
Negative
Error signal
$-V_{eye}$
$V_{eye}$
$V_{image}-V_{eye}=V_{eye}$
Eye movement
B
$\leftarrow V_{oks}$
$\rightarrow V_{image}= V_{oks} + 2 \times V_{eye}$
Healthy Subject
Misrouted Patient
Healthy Subject
Feedback
Negative
Positive
Negative
Error signal
$V_{oks}-V_{eye}$
$V_{oks}+V_{eye}$
$V_{image}-V_{eye}=V_{oks}+V_{eye}$
Eye movement

**Figure 3.**

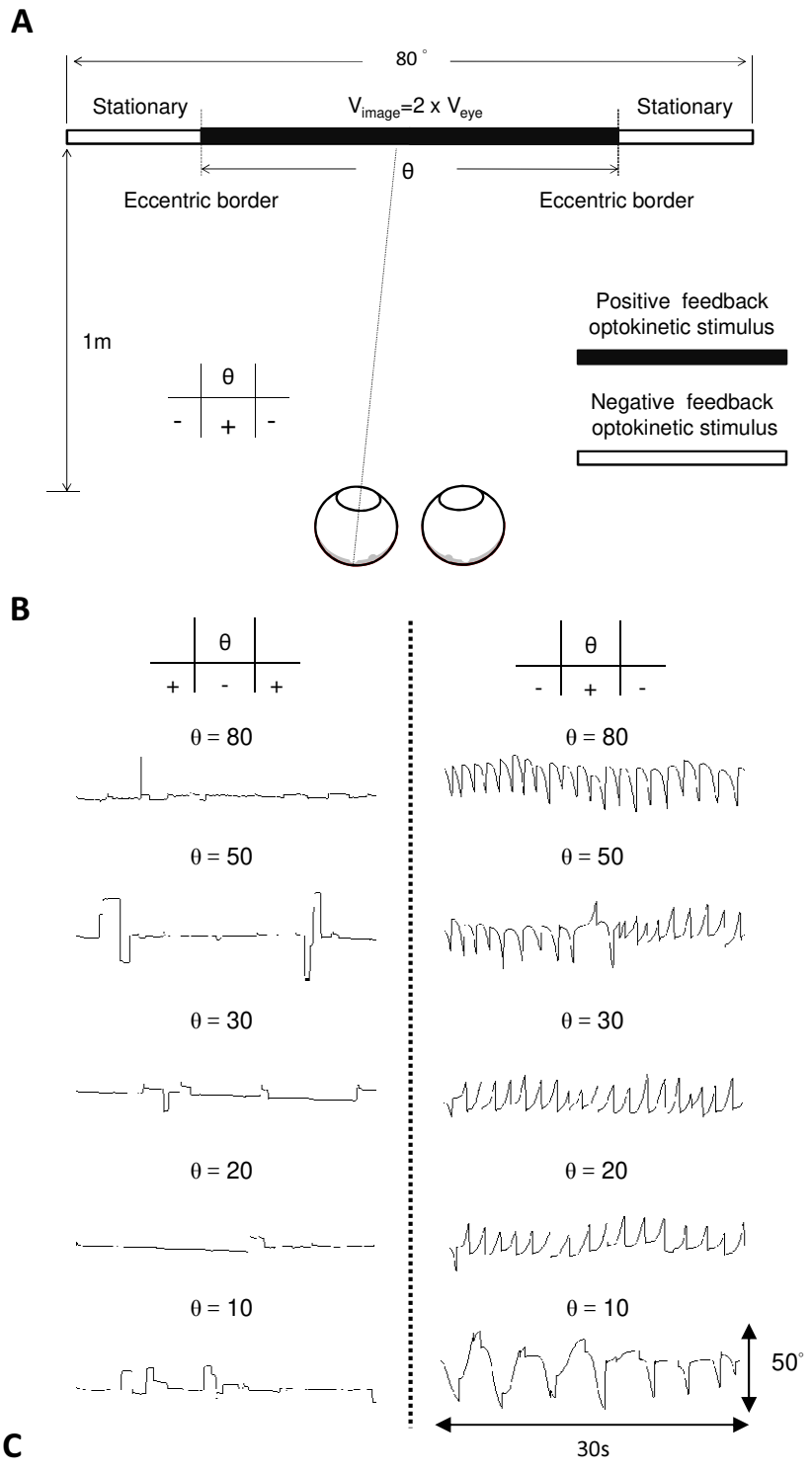
A
80 °
Stationary
$V_{image}$=2 x $V_{eye}$
Stationary
θ
Eccentric border
Eccentric border
1m
θ
- + -
Positive feedback optokinetic stimulus
Negative feedback optokinetic stimulus
B
θ
+ - +
θ
- + -
θ = 80
θ = 50
θ = 30
θ = 20
θ = 10
50°
30s
C
Median absolute eye velocity (deg/s)
0
4
8
12
16
20
80 50 30 20 10 10 20 30 50 80
θ
+ - +
θ
- + -

**Figure 4.**

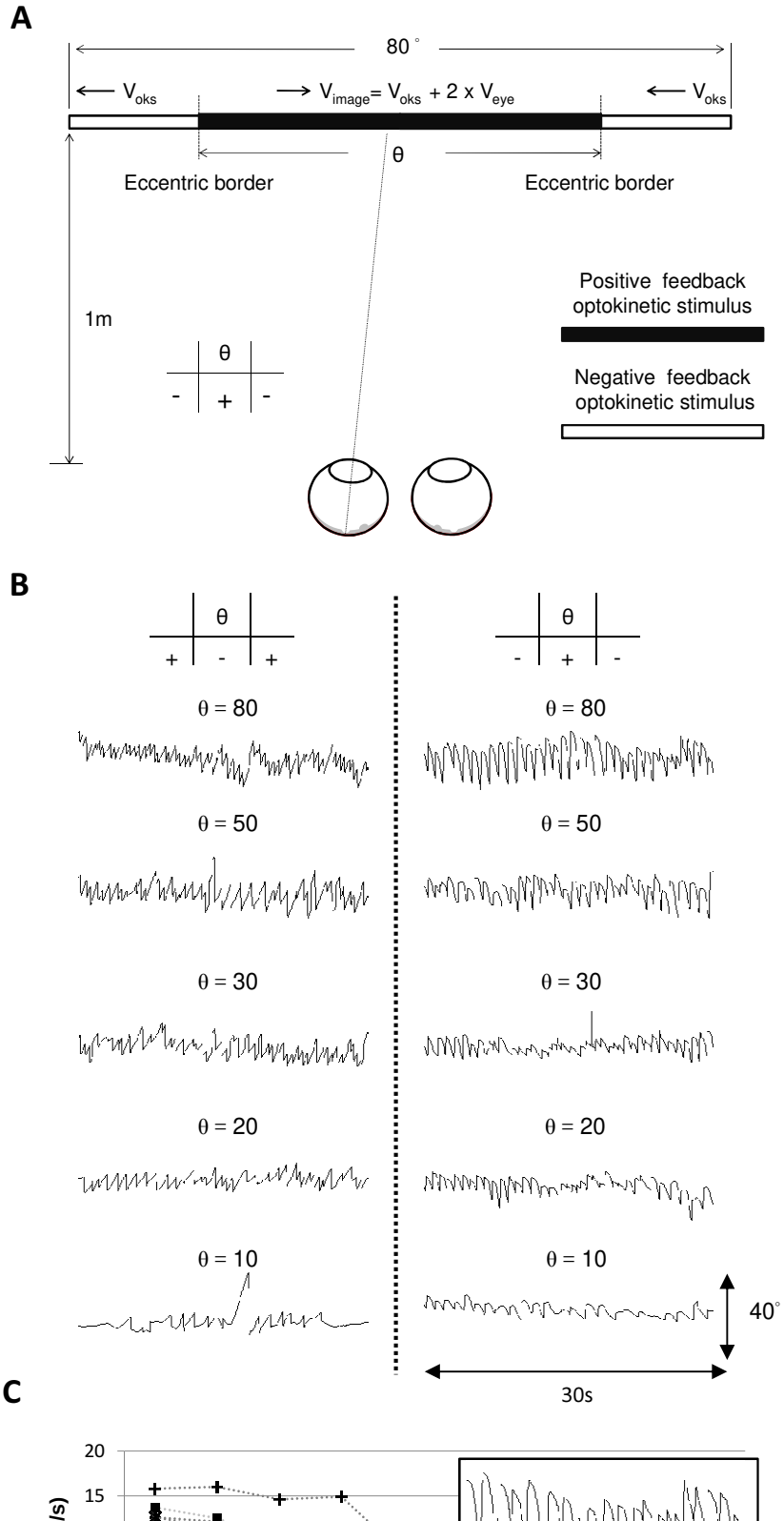
A
80 °
V_oks
V_image= V_oks + 2 x V_eye
V_oks
θ
Eccentric border
Eccentric border
1m
θ
- + -
Positive feedback optokinetic stimulus
Negative feedback optokinetic stimulus
B
θ
+ - +
θ
- + -
θ = 80
θ = 50
θ = 30
θ = 20
θ = 10
40°
30s
C
Median eye velocity (deg/s)
20
15
10
5
0
-5
-10
-15
-20
80 50 30 20 10 10 20 30 50 80
θ
+ - +
θ
- + -

**Figure 5.**

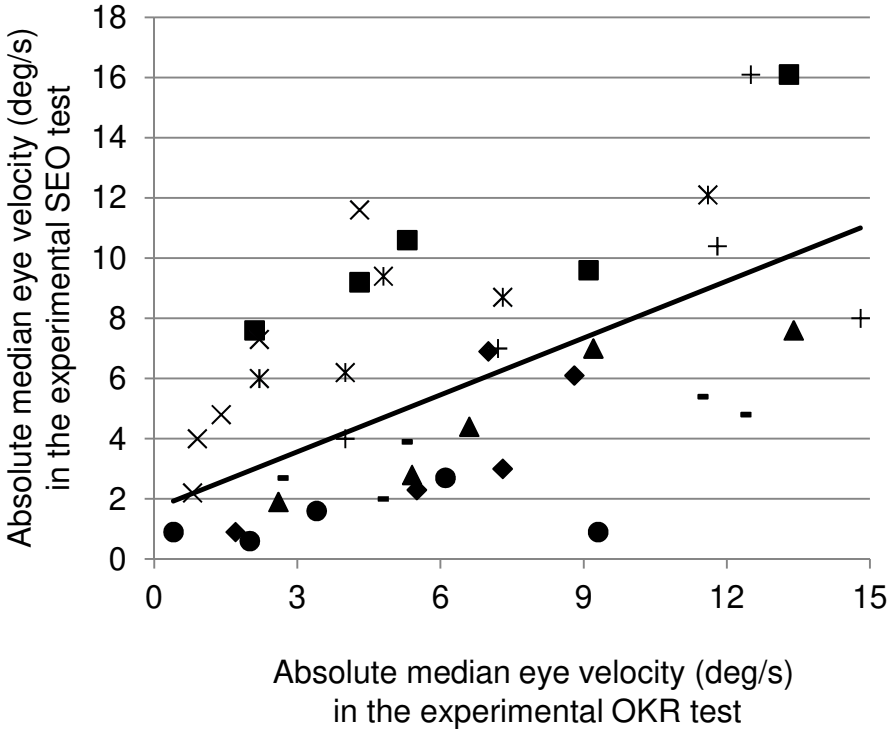
Absolute median eye velocity (deg/s) in the experimental SEO test
18
16
14
12
10
8
6
4
2
0
0
3
6
9
12
15
Absolute median eye velocity (deg/s) in the experimental OKR test

**Figure 6.**

**A**

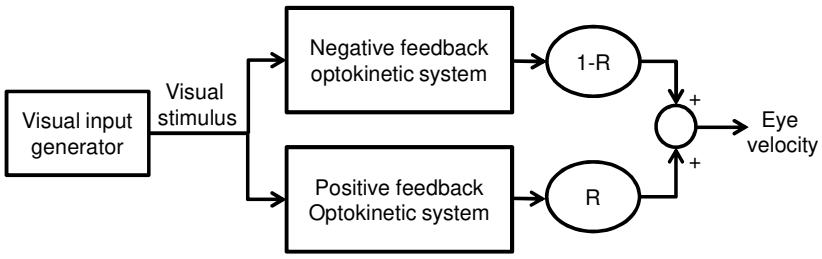
Visual input generator
Visual stimulus
Negative feedback optokinetic system
Positive feedback Optokinetic system
1-R
R
+
+
Eye velocity

**B**

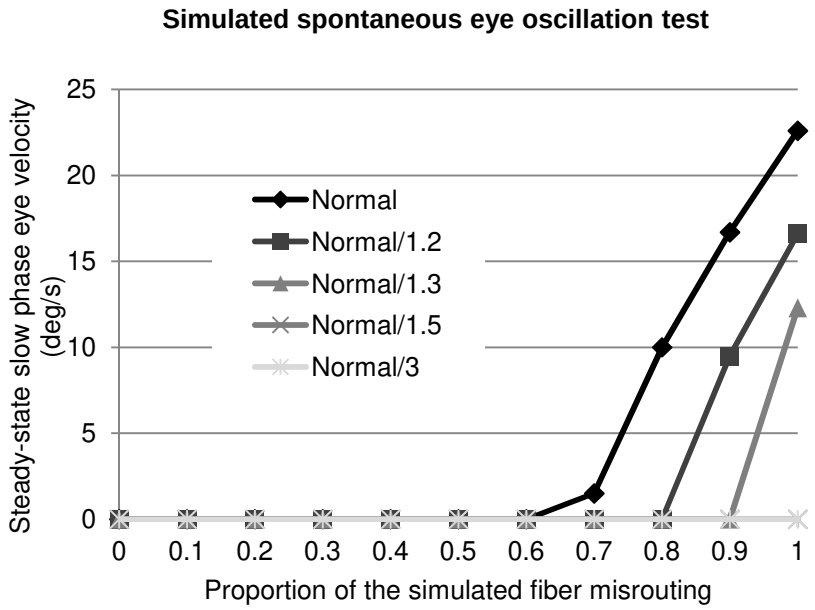
Simulated spontaneous eye oscillation test
Steady-state slow phase eye velocity (deg/s)
25
20
15
10
5
0
Normal
Normal/1.2
Normal/1.3
Normal/1.5
Normal/3
0
0.1
0.2
0.3
0.4
0.5
0.6
0.7
0.8
0.9
1
Proportion of the simulated fiber misrouting

**C**

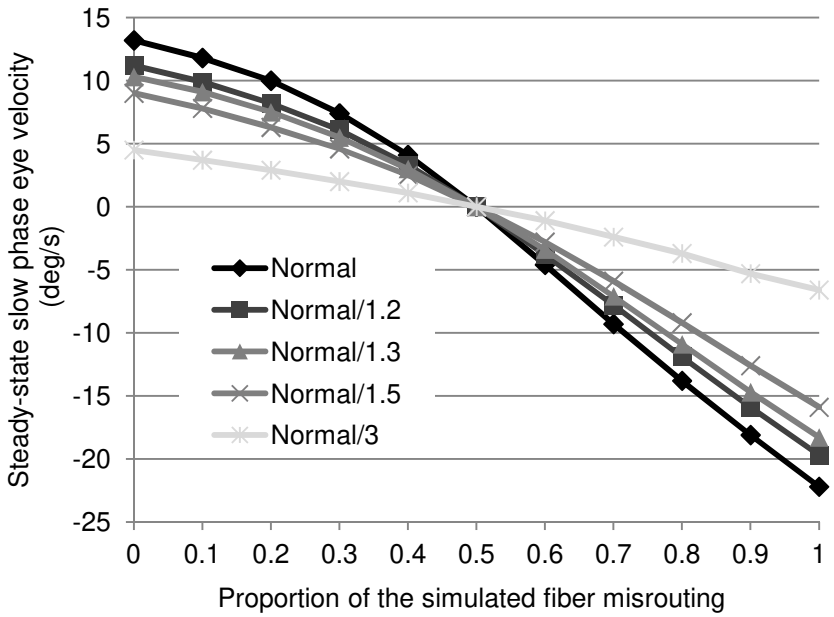
Simulated optokinetic response test
Steady-state slow phase eye velocity (deg/s)
15
10
5
0
-5
-10
-15
-20
-25
Normal
Normal/1.2
Normal/1.3
Normal/1.5
Normal/3
0
0.1
0.2
0.3
0.4
0.5
0.6
0.7
0.8
0.9
1
Proportion of the simulated fiber misrouting

**Figure 7.**

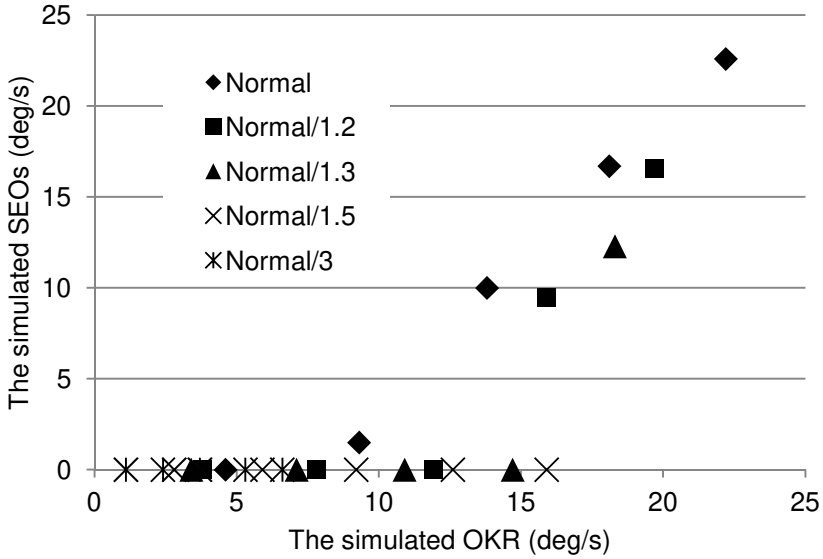
25
20
15
10
5
0
0
5
10
15
20
25
The simulated SEOs (deg/s)
The simulated OKR (deg/s)
Normal
Normal/1.2
Normal/1.3
Normal/1.5
Normal/3